

# The role of space science in space weather specification: An illustration with auroral studies\*

Chanchal Uberoi

*Space weather predictions and forecasts are now understood to be essential for protection of both the ground-based and space-based technical systems from their hazardous effects. In this article an attempt is made to point out the importance of the role of space science community in the starting of a National Space Weather Service, by exemplifying the specifications made about the ionospheric conductivity from the recent auroral studies.*

SPACE weather is a relatively new phrase in space physics. It refers broadly to conditions in space that may affect human activities. These conditions are changing all the time. Differing types and intensities of solar activity produce different conditions in the solar wind, which in turn has an impact on the conditions in the magnetosphere, ionosphere and upper atmosphere. Adverse space weather conditions, just like atmospheric weather, arise due to geomagnetic storms. It covers all particle, electromagnetic and ionospheric disturbances resulting from solar magnetic storms, coronal mass ejections, fast solar wind streams and ionospheric instabilities. The space weather can have deleterious impact on the space-based as well as ground-based technical systems. These are summarized below.

## Ionosphere effects

These include: (1) Radio propagation; (2) communication; satellite signal interferences; (3) induction of electrical currents in the earth – (a) power distribution systems; (b) long cables; and (c) pipelines.

## Radiation effects

These include: (1) Solar cell damage; (2) semiconductor damage and failure; (3) spacecraft charging; (4) astronaut safety; and (5) airline passenger safety.

## Magnetosphere currents

These include attitude control of communication spacecraft.

These impacts resulting in failure of power systems and space systems can cause losses in millions of dollars, besides causing difficulties for the public. Hence, research in space weather has become important and a challenging area in space physics.

There are two aspects to space weather research. One is to have specifications about the plasma and magnetic field parameters of solar wind, interplanetary medium and magnetosphere-ionosphere plasma systems and the specifications of solar energetic particle environments and magnetospheric radiation conditions. The other aspect is to forecast and nowcast solar energetic events, magnetospheric disturbances and ground-induced currents, magnetospheric radiation fluxes, ionospheric and thermospheric disturbances. These are necessary, if in future, we would like to get the space weather forecast maps for the inner magnetosphere (Figure 1) to protect our spacecrafts and communication systems.

Figure 1 shows a familiar weather map from the Weather Channel and a fictional version of what a comparable 'space weather' map might resemble<sup>1</sup>. Analogous to traditional weather maps, the objective is to take data from an array of monitors and to synthesize those data into a picture of the space environments. Instead of cloud cover or barometric pressure, space weather maps need to display particle fluxes and plasma temperatures and densities. In place of cold fronts we need to represent the locations of boundaries such as the magnetopause or plasmasphere. A number of approaches to producing space weather maps are possible, each with its particular strength and weakness.

For starting a National Space Weather Service (NSWS) just like the National Weather Service as pointed by Siscoe *et al.*<sup>2</sup>, the following six elements are necessary:

1. Space Environment Services Center (SESC), which forecasts and monitors geomagnetic storms and radiation hazards.
2. Continuous, real-time reception of essential data. Till now energetic particle, solar X-ray, magnetic field,

Chanchal Uberoi is in the Department of Mathematics, Indian Institute of Science, Bangalore 560 012, India.

e-mail: cuberoi@math.iisc.ernet.in

\*Based on the talk given by the author during the workshop on 'Space Weather and ACE Real-time Data' at ISRO.

trapped particle and precipitating particle data from the geostationary operational environmental satellite (GOES), television and infrared observing satellite (TIROS), defence meteorological satellite programme (DMSP) were being received.

A crucial input for magnetospheric and ionospheric forecasting, that is upstream measurements of solar wind parameters, including the interplanetary magnetic field (IMF) were missing, but now these data can be secured from the Wind and Advanced Composition Explorer (ACE) spacecraft. This quasi-continuous, real-time solar wind and IMF data came at the right time, close to the solar maximum in 2001.

3. Another infra-structural element is numerical forecasting – Numerical specification and forecast algorithms have to be put in operation.
4. Personnel to interpret the data and serve the customers.
5. Another element emphasized in this article is an involved scientific community. Large expenditure

has gone in to support research in space physics and aeronomy. A mature science now exists to interpret space weather phenomena, develop specification and forecast algorithms and establish new predictive models and data sources.

6. To find suitable customers.

The near-earth space environment, the magnetosphere, is loaded with energy from the interaction with the highly variable solar wind. Part of this energy is in turn dissipated by particle precipitation into the ionosphere, giving auroral display<sup>3</sup>. The auroras are therefore the most fascinating manifestation of the energy coupling between the solar wind and magnetosphere–ionosphere system (Figure 2). The study of auroras is therefore of fundamental importance to understand the inflow, storage, reconfiguration of energy release events and thus is important in the space weather research. To illustrate this, I shall point out some very interesting recent findings in the study of auroral arc formation. The interpretation of

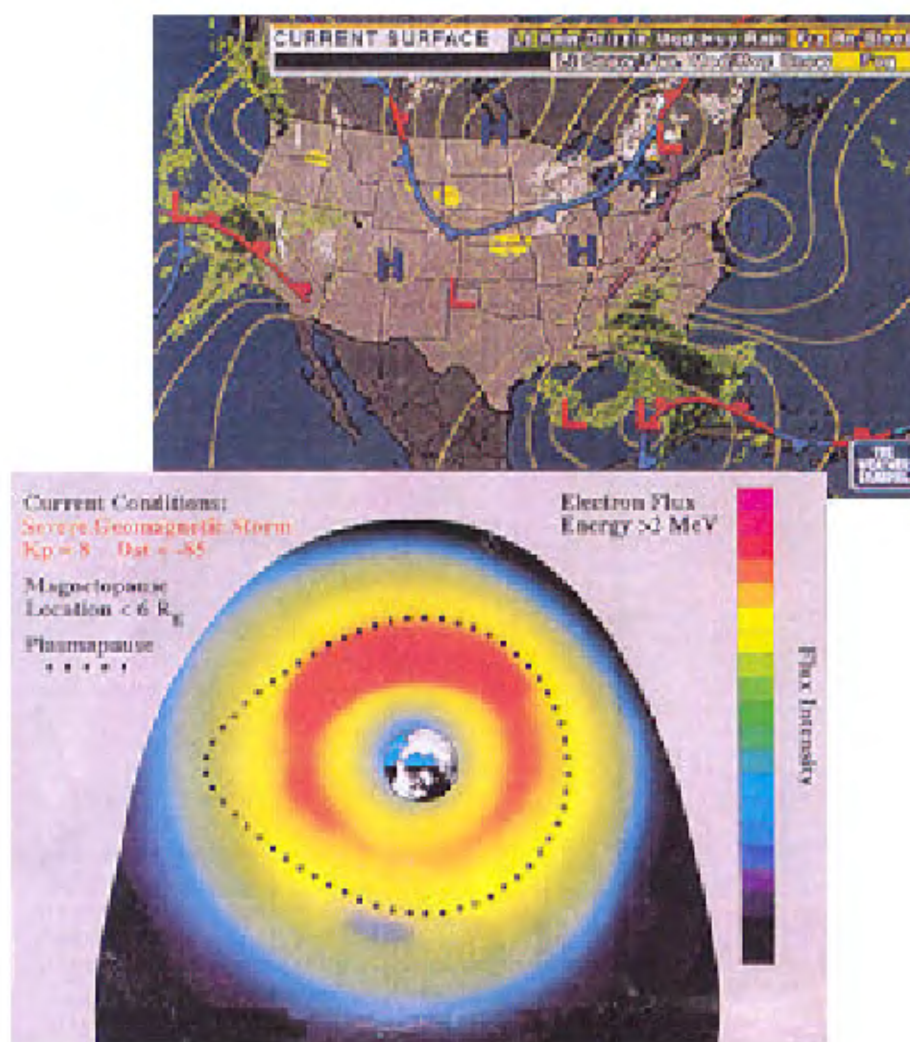


**Figure 1.** A familiar surface weather map from The Weather Channel and a fictional version of what a comparable 'space weather' map might resemble (after ref. 1).

these results by space physicists shows that these findings can have implications for the predictability of space weather.

## Rare events of ‘great aurorae’

The relationship between the phenomenon of aurora and the space weather disturbances is very old. To review some of the events will be interesting. Carrington saw and recorded the first solar flare on 1 September 1859, Stewart observed the violent magnetic storm a day or two later. Intense auroral displays were seen from the tropics during this period and at the same time, telegraph operators commented that it was possible to operate the telegraph system without battery supply. The potential drops generated by the (observed) aurora provided sufficient power. It was also in this year that for the first time, Whistler signal was reported to be interfering with the radio communication.

We also have an interesting record of an unusual aurora being observed in the tropics of Bombay as well as in many other parts of India on 4 February 1872. It was also seen in Egypt and elsewhere. It was associated with an equal outstanding magnetic storm.

During the International Geophysical Year in 1957, the three greatest storms occurred. The aurora was seen from Mexico city in the tropics. One of the storms occurred on 13 September 1957. Another occurred on 10/11 February 1958; this storm seems to have been compounded of two substorms, so much so that interestingly, between the two substorms, the auroral electrojet almost died away, and at these times the aurora could not be seen even from Alaska, a region of frequent aurora visibility. The aurora was again visible from Alaska to southern USA, when the second substorm became active.

The auroral activity in the year 1989, last solar maximum, was tremendous<sup>4</sup> and this leaves us with the

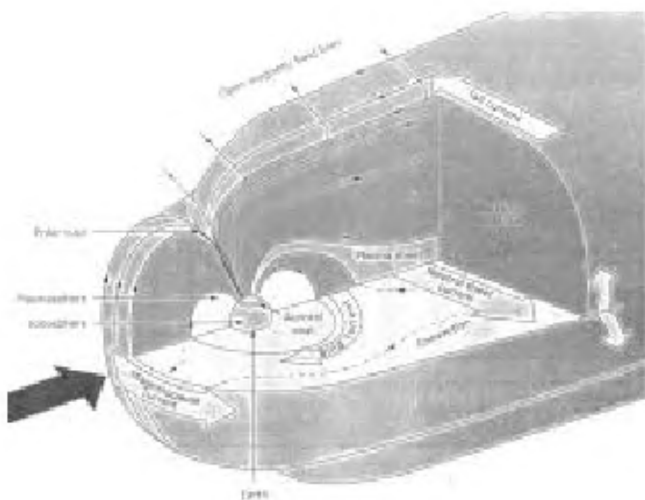


**Figure 2.** Solar wind and magnetosphere–ionosphere system.

understanding that we can expect such activity during the forthcoming solar maximum. During 6–14 March 1989, several crossings of GOES showed that the magnetopause typically located at  $10 R_E$  distance, moved inside the geostationary orbit ( $6.6 R_E$ ) and it was within this orbit approximately for 3.2 h. These episodes comprise the longest duration compression observed by the GOES satellites from 1976 to 1989.

Magnetic substorms were occurring in the auroral zone before the particles from the 6 March flare arrived on the earth. The ‘great magnetic storm’ began on 13–14 March (Figure 3). It appears that auroral electrojet was located over Central USA for several hours. This is consistent with the Dynamic Explorer (DE) auroral imagery and a similar image taken by satellite F9 of the DMSP series around 0355 UT on 14 March. The auroral electrojet index, AE, showed the intensity of the auroral zone substorm ranging from zero to as large as 3000 nT (Figure 4).

Extremely large auroral zones were seen. Figure 5 shows DEL images from two separate passes over the Antarctic, six years apart and recorded from similar viewpoint. It shows the quiet auroral oval at 1623 UT on 22 March 1983 and enormously expanded auroral oval at 1826 UT on 13 March 1989.

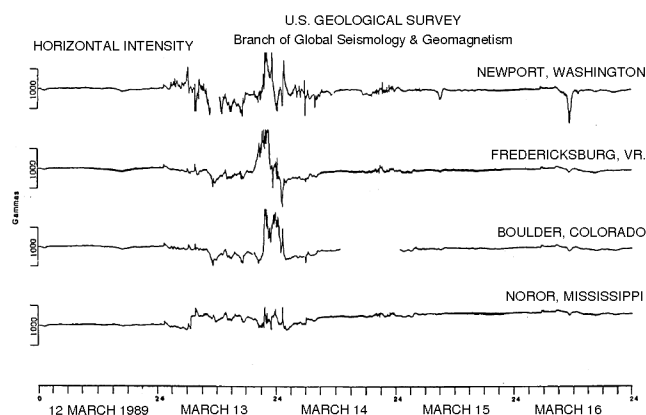


**Figure 3.** Mid-latitude magnetometers measuring auroral currents (many going off-scale) (after ref. 4).

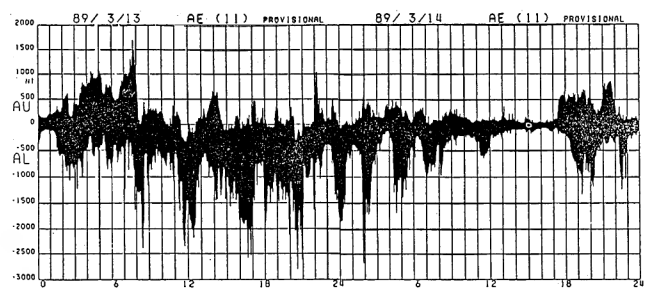


**Figure 4.** Provisional auroral electrojet indices for 13–14 March 1989. The AE index =  $Au - Al$ ; however, this must be considered a lower limit since the auroral currents were well equator-ward of the typical auroral zone stations and even so many were saturated (after ref. 4).

Aurorae viewing reports came from several ground observations. Brilliant aurorae were seen across the US on the nights of Sunday–Monday 12–13 March. Red aurorae from Florida, Mexico and London were reported. Southern Australia was under cloud-cover, but North Australia reported the observation.

### Three intense aurorae occurring in majority

The oldest documented relationship between the number of sunspots (the solar cycle) and terrestrial effects is the increased frequency of aurorae in the period immediately after the solar maximum. This correlation, as we have already seen, appears to be based only on observations of the relatively rare events of ‘great aurorae’, which are those that reach mid-latitudes or lower. The overwhelming majority of intense aurorae, and therefore most of the energy input into the ionosphere, occur at high latitudes, where aurorae appear every night over a wide region of high latitudes (intense aurorae: the threshold criterion is  $5 \text{ erg cm}^{-2} \text{ s}^{-1}$ ; the threshold of visibility with the unaided eye is  $\sim 1 \text{ erg cm}^{-2} \text{ s}^{-1}$ ). Therefore, the *great auroral systems* that happen a few times in a year contribute only negligibly to the total energy input into the upper atmosphere. Hence, it is of intrinsic value both from the point of view of importance of the auroral energy flux input to upper-atmospheric high-latitude chemistry and for understanding the physics of auroral arc formation to study the effects of solar cycle on the global frequency of intense aurorae. Specifically, there is recent research supporting the idea that discrete aurorae are suppressed by sunlight where background conductivity of the ionosphere is high, thus in turn supporting the idea that ionospheric conduc-

tivity is a crucial determinant of whether intense auroral arcs form or not. Here, I first define the ‘discrete’ and ‘diffuse’ aurora.

### Discrete and diffuse aurorae

Aurorae are often characterized as being discrete or diffuse. Originally, these terms were derived from the appearance of the aurora in satellite images such as ISIS or DMSP, but gradually physical mechanisms have been associated with the terms.

Charged particles from space, mainly electrons and protons, constantly precipitate along geomagnetic field lines into the earth’s upper atmosphere at high latitudes. Most of this precipitation and the auroral airglow it produces is diffuse, representing a *direct dumping* of various space plasma populations that surrounded the earth. These are *diffuse auroras* and are associated with energetic electrons and protons precipitated from magnetospheric trapped particle populations (Figure 6 a).

But, at times the electrons show clear signs of magnetic field-aligned acceleration by hundreds of eV or occasionally even a few tens of keV. The result is a characteristic profile in the electron spectra: sometimes loosely called monoenergetic because of the sharp energy-flux peak at the acceleration energy. Discrete aurorae (Figure 6 b) correspond to such accelerated beam of electrons. These are brighter and more intense type of aurorae, which are bright arcs, rays or curtains, narrow in latitude and elongated in longitude. Discrete aurorae can be studied optically only in dark conditions, whereas accelerated electrons can be measured by satellite at any time.

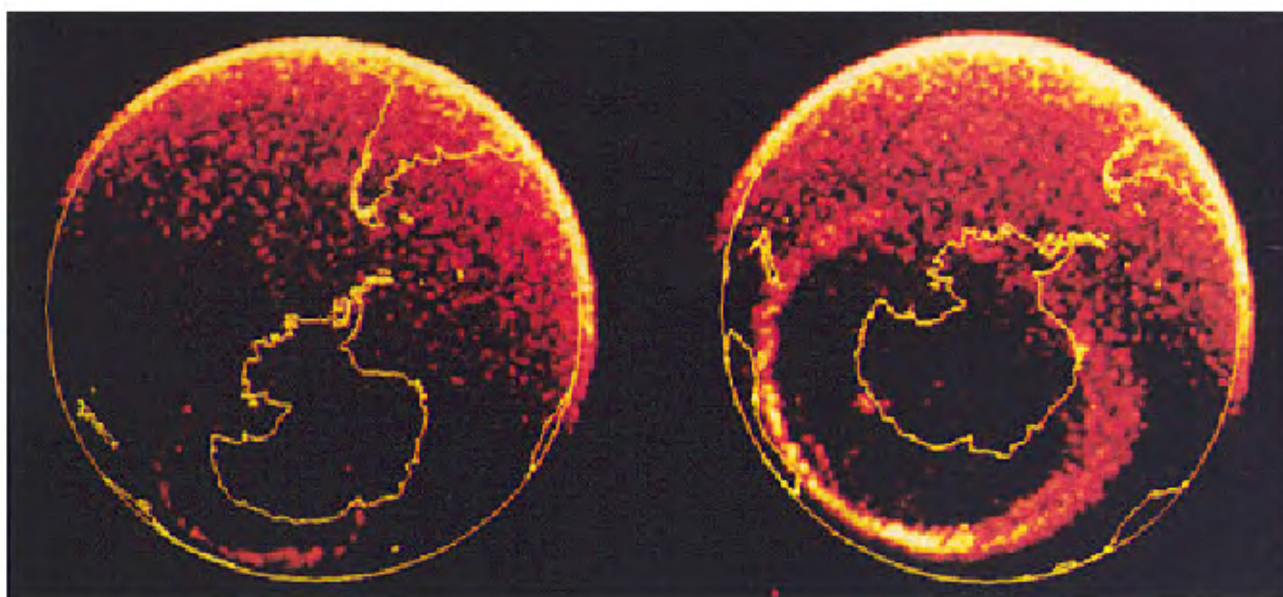


**Figure 5.** Southern hemisphere DE1 ultraviolet images. (Left) Quiet-time auroral ring (taken at 1623 UT on 22 March 1983); (Right) Largest auroral zone ever recorded by the spacecraft, taken at 1826 UT on 13 March 1989.



### Frequency of intense aurorae in sunlight and darkness

In 1996, Newell *et al.*<sup>5</sup> presented a statistical study of electron precipitation events by using nine years (1984–



**Figure 6.** *a*, Diffuse aurora; *b*, discrete aurora.

1992) of charged-particle data from weather satellites belonging to the DMSP series. Their results presented a first surprising report that there is a large difference between the frequency of intense aurorae in sunlight and in darkness. The intense electron acceleration events with energy flux above  $5 \text{ ergs cm}^2 \text{ s}^{-1}$  in the dusk-to-midnight sector was three times more likely in local darkness (solar zenith angle  $> 100^\circ$ ) than in sunlight (solar zenith angle  $< 85^\circ$ ). Figure 7 illustrates the effect of sunlight on the frequency of intense electron acceleration event. Although the electron acceleration event can be observed at all local times and at almost all latitudes, the large majority of intense events occurs in the 1800–2400 magnetic local time (MLT) sector, where neither sunlight nor diffuse auroras supplies significant background ionospheric conductivity.

Very recently, four additional studies using widely different approaches have arrived at the same result concerning the frequency of intense aurorae with respect to sunlight. These are: (1) EMIC – electromagnetic ion-cyclotron waves; (2) auroral kilometric radiation; (3) Riometer absorption; (4) polar satellites for global ultraviolet images; (5) solar cycle variation of aurora.

### Solar cycle variation of aurora

Now we come to the study of intense auroral events on a global scale in both darkness and sunlight over the period of a solar cycle. This was conducted by Newell *et al.*<sup>6</sup> by using the electron detectors on-board satellites of DMSP. They investigated the frequency of intense electron acceleration events. Electron acceleration events are characterized by ‘mono-energetic’ electron spectra with precipitating energy flux above  $5 \text{ ergs cm}^2 \text{ s}^{-1}$ , and their association with aurora was established by direct rocket shots into visible aurorae as a function of solar cycle and explicitly as a function of F10.7 by using twelve years of DMSP

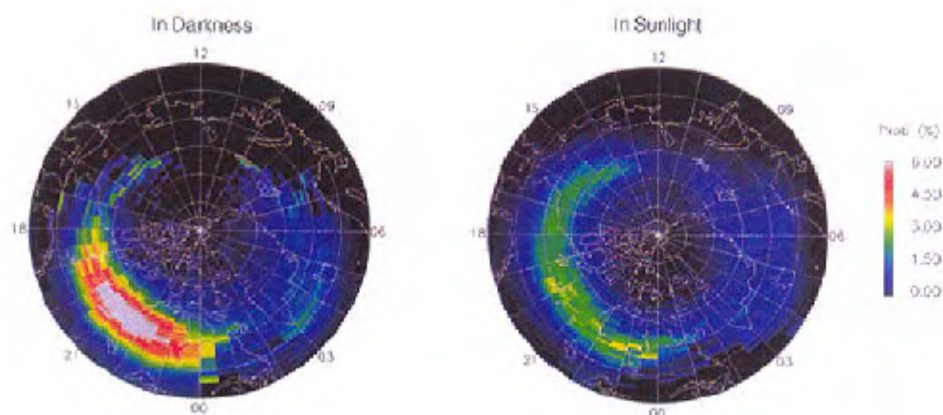


**Figure 7.** Intense discrete aurorae occur much more frequently in darkness than in sunlight. This effect is attributed to the increase in ionospheric conductivity caused by sunlight. The probability of observing intense discrete auroras ( $> 5 \text{ ergs cm}^2 \text{ s}^{-1}$ ) in corrected magnetic coordinates with the continental outlines are shown at 06:00 UT (after ref. 5).

particle-precipitation data (1984–1995) comprising approximately  $2 \times 10^8$  individual spectra. Binning auroral frequency explicitly by F10.7 produced the clearest results and since most intense electron acceleration occurs in the dusk-to-midnight sector, only this region was considered.

### Yearly averages

Figure 8 shows the variation of intense auroral events over the course of a solar cycle. Figure 7 shows plots with measurements taken under sunlit and dark conditions. Local time of measurement is 18:00 to 24:00 MLT, the sunlit measurements occur during local summer months. It is noted that:

- (1) The sunlit hemisphere measurements seem to show a relatively clear solar cycle variation, with a pronounced minimum in auroral frequency around the solar maximum.
- (2) Under conditions of darkness, no clear solar cycle

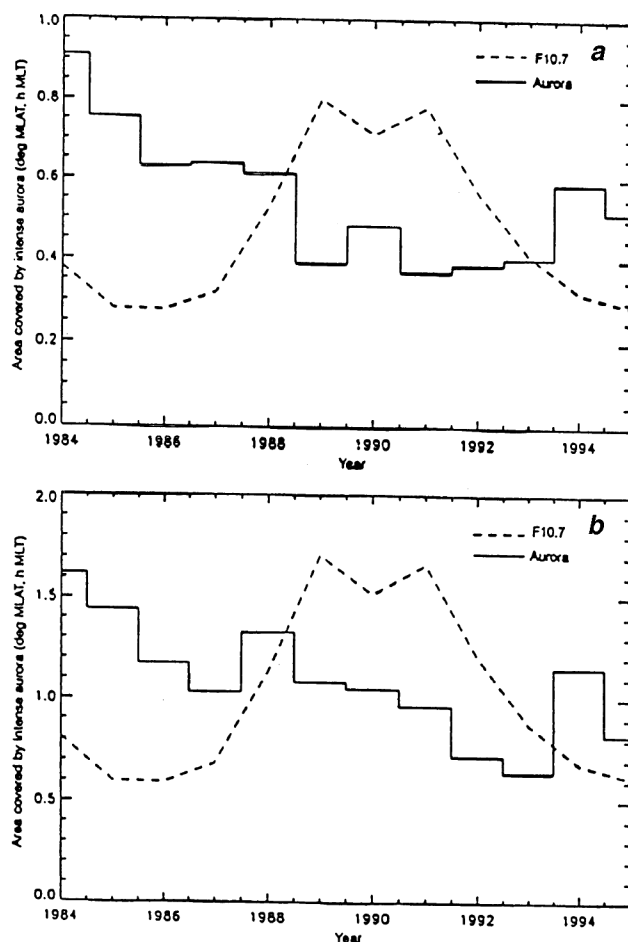


**Figure 8.** Mean surface area covered by intense ( $\geq 5 \text{ erg cm}^{-2} \text{ s}^{-1}$ ) aurorae over a 12-year period. For comparison, the F10.7 number which correlates well with solar cycle and is often used as a proxy for solar activity, is also plotted (broken line). *a*, Locally sunlit conditions (solar zenith angle  $\leq 85^\circ$ ); *b*, Conditions of local darkness (solar zenith angle  $\geq 110^\circ$ ) (after ref. 6).

trend exists (at least from the 12-year stretch of data).

### Variation with F10.7

Although the yearly averages are of intrinsic interest, this approach is not the best for determining whether ionizing solar radiation is involved directly in suppressing the formation of intense aurorae. Over the course of a year, both the frequency of aurorae and the F10.7 number can undergo substantial variations. Figure 9 shows variations with the values of F10.7 at the time of observation.

Each data point represents the time-averaged occurrence rate of aurora over the 12-year period, 1984–1995, such that the daily F10.7 number was within the appropriate bin. It is seen that under sunlit conditions there is high-degree precision with correlation coefficient of  $-0.96$  and under dark conditions there is no correlation ( $-0.01$ ).

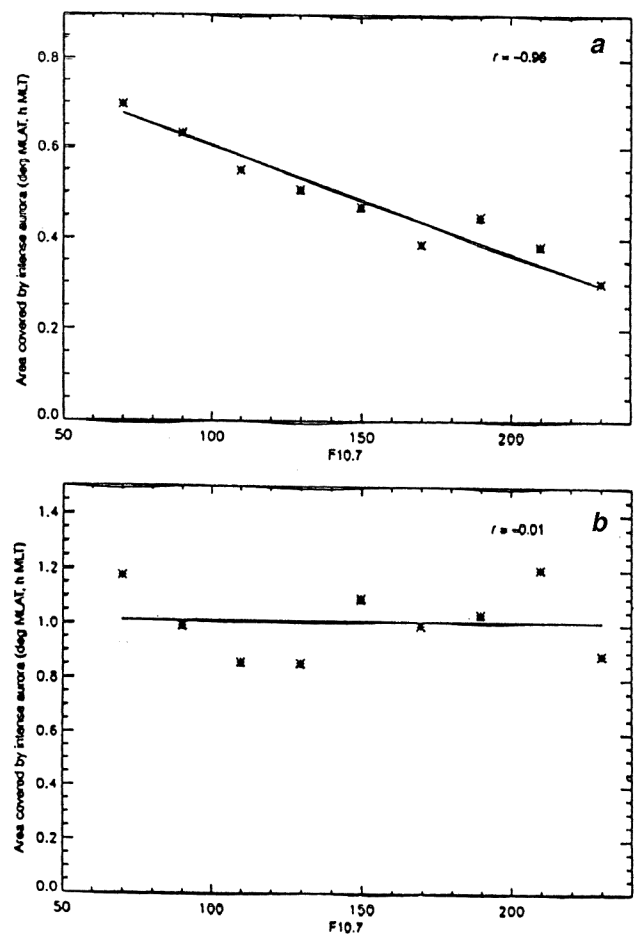


**Figure 9.** Mean surface area covered by intense auroral area as an explicit function of F10.7 daily value, which is a proxy for ionizing solar radiation, *a*, Sunlit conditions (solar zenith angle  $\leq 85^\circ$ ); *b*, Local conditions of darkness (solar zenith angle  $\geq 110^\circ$ ) (after ref. 6).

Taken together, these results are a powerful evidence that it is not some hidden variable indirectly related to solar cycle (such as solar wind velocity or density) that produces the F10.7 effect, but the presence of ionizing solar radiation itself.

Statistical studies have now amply demonstrated that background ionospheric conductivity is a crucial determinant of whether intense auroral arc form. In retrospect this is not very surprising! A fluorescent light will not fluoresce if a highly-conducting alternate path, such as a piece of copper wire exists. However, these new findings did surprise the space physics community.

The new findings that intense aurorae are suppressed in sunlight compared to darkness supported by five additional statistical studies<sup>7</sup> as mentioned above and that the global occurrence rate of intense aurorae is actually slightly lower at the solar maximum than at the solar minimum has led the scientific community to endorse the ionospheric feedback mechanism<sup>8</sup> for auroral arc formation<sup>9</sup>. The dynamics of magnetospheric plasma, including magnetic substorms, requires geomagnetic field-aligned currents driven from near-earth space, into, across and out of the ionosphere. The ionospheric conductivity feedback hypothesis starts by noting that an unstable situation exists when insufficient conductivity exists in the ionosphere to support these imposed currents. The rapidly changing density gradients that exist above the ionosphere can make electromagnetic wave resonances possible. The resulting acceleration of electrons to keV energies creates

sufficient ionospheric conductivity to complete the circuit. Moreover, once a localized region of enhanced ionospheric conductivity is started, more current is directed towards that region, carried by additional precipitating electrons, which then further enhance the localized conductivity (see Figure 10).

### Polar UV images: Measure of energy output of the magnetosphere

A very important study of auroral images using the polar UV imager has been reported recently by Lui *et al.*<sup>10</sup>. More than 9000 satellite global images of aurorae taken in January 1997 have been used to monitor the energy output over the entire magnetospheric system directly. Though previously it has been established that on the smallest scale, such as fine auroral arcs of width 100 m, the power output depends on the details of magnetosphere-ionosphere coupling, while on the largest scale, the global auroral power which averaged over an hour or so correlates well with solar wind input, there has been no investigation on all scales. In this study, the probability distribution of

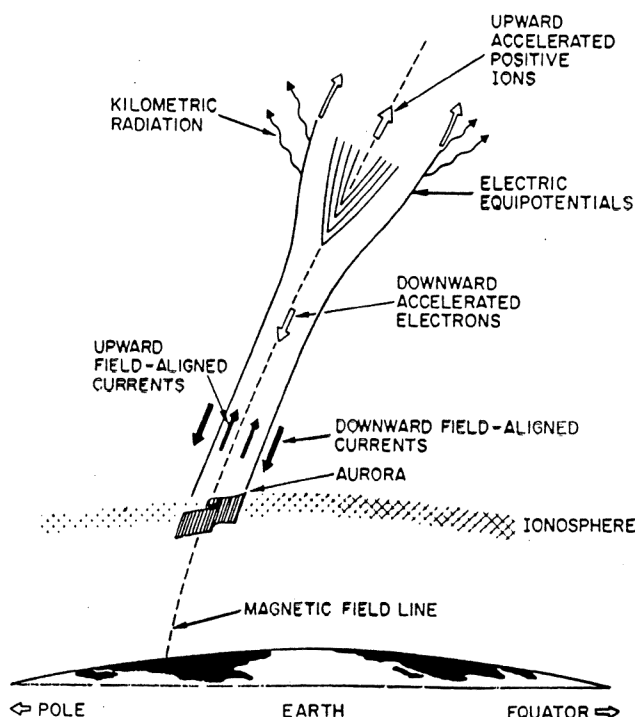


**Figure 10.** Auroral-arc action: Field-aligned currents, parallel electric field and particle-acceleration region, and kilometric-radiation phenomenon associated with an auroral arc above a polar region (after ref. 9).

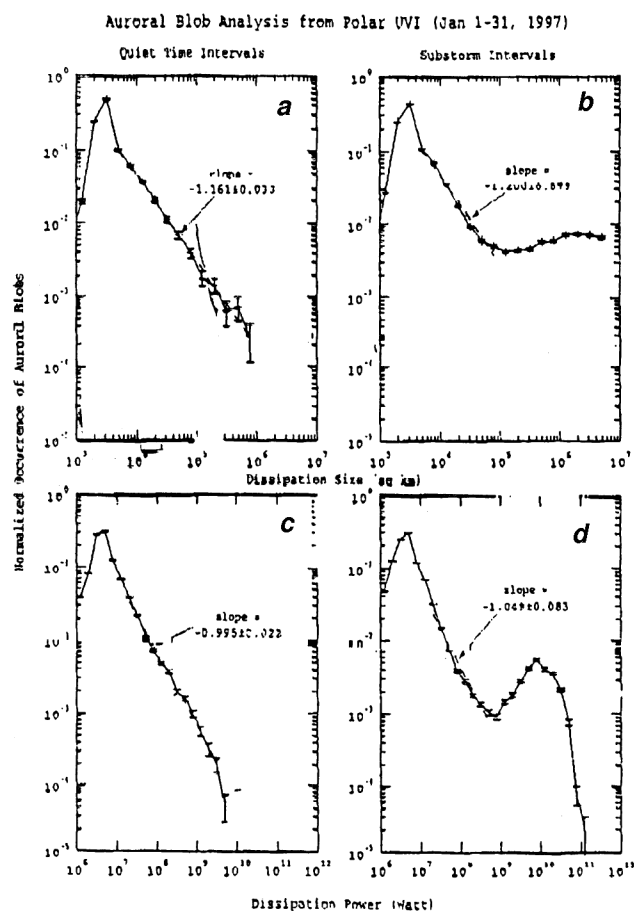


**Figure 11.** Probability distribution of size and power output of individual auroral region. Size distribution during (a) quiet times and (b) substorms. Power distribution during (c) quiet times and (d) during substorms (after ref. 10).

spatial size and energy dissipated by the magnetospheric system for all scale sizes have been obtained. Figure 10 shows the distribution of the dissipation power indicated by the auroral blob intensity. These distributions resemble remarkably well the size distributions of the auroral blobs given in the same figure.

During quiet time (Figure 11 *c*) the dissipation power has a power law with a slope of approximately  $-1$ . Similarly there is a peak in the distribution for substorms (Figure 11 *d*) at the dissipated power exceeding  $\sim 5 \times 10^8$  W. Between  $\sim 5 \times 10^6$  and  $\sim 5 \times 10^8$  W, the distribution has a slope of again nearly  $-1$ .

The power law distribution and the similarity in the slope value for both the size and dissipated power of events for quiet time and for substorms led to the suggestion that the dynamic magnetosphere resembles a simple avalanche system, implying that the coupled solar wind–magnetosphere system is out of equilibrium, dissipating energy via avalanches (or sandpile model) which have no intrinsic scale. These are only suggestions; the only other comment which can be made is that a class of such systems is in a self-organized critical state. The onset of local avalanches in the sandpile model can be physically related to the merging of coherent structures and Alfvén resonances or current disruption by kinetic instabilities in the magnetotail.

## Conclusions

These auroral studies have shown that the characterization of global energy transport in the solar wind–magnetosphere–ionosphere is of fundamental importance in under-

standing the magnetospheric or space weather dynamics. The solar wind is a source of kinetic energy and magnetic flux which is transferred to and stored in and then released from the magnetosphere. Understanding the physics and mathematics of the solar energy coupling to magnetosphere–ionosphere system will certainly improve the forecast codes by the NSWS. Also NSWS needs support from space science community in the form of new empirical approaches to space environment specification and forecasting.

Finally, I would like to add that to get active support and participation from scientists, the space science community should be familiarized with space weather impacts on the society and the space weather forecasting procedures and codes.

1. Reeves, G., Friedel, R. and Hayes, R., *EOS*, 1998, **79**, 613–617.
2. Siscoe, G., Hildner, E., Killeen, T. L., Lanzerotti, L. J. and Lotko, W., *EOS*, 1994, **75**, 365–367.
3. Uberoi, C., *Earth's Proximal Space*, Universities Press India Ltd., 2000.
4. Allen, J., Frank, L., Sauer, H. and Reiff, P., *EOS*, 1989, **70**, 1479–1486.
5. Newell, P. T., Meng, Ching-I. and Lyons, K. M., *Nature*, 1996, **381**, 766–767.
6. Newell, P. T., Meng, Ching-I. and Wing, S., *Nature*, 1998, **393**, 342–344.
7. Newell, P. T., *EOS*, 1998, **79**, 625–628.
8. Lysak, R. L., *J. Geophys. Res.*, 1991, **96**, 1553–1568.
9. Borovsky, J. E., *J. Geophys. Res.*, 1993, **98**, 6101–6138.
10. Lui, A. T. Y., Chapman, S. C., Liou, P. K., Newell, T., Meng, C. I., Beittsacher, M. and Parks, G. K., *Geophys. Res. Lett.*, 2000, **27**, 911–914.

Received 3 May 2001; revised accepted 10 July 2000